September 15, 1997

EXPERIMENTAL PROPOSAL FOR GSI/SIS

SEARCH FOR BOUND η- AND ω-NUCLEAR STATES USING RECOILLESS (d,^{3}He) REACTION AT GSI-SIS

– Study of Meson Mass Shift in Nuclei –

R.S. Hayano[1] , K. Itahashi, T.M. Ito, K. Oyama, K. Tanida
Department of Physics, University of Tokyo, Hongo, Bunkyo-ku, Tokyo 113, Japan

M. Iwasaki
Department of Physics, Tokyo Institute of Technology, Ookayama, Meguro-ku, Tokyo 152, Japan

H. En'yo
Department of Physics, Kyoto University, Kyoto, Japan

S. Hirenzaki
Department of Physics, Nara Women's University, Nara 630, Japan

H. Toki
RCNP, Osaka University, Osaka 567, Japan

H. Gilg, A. Gillitzer[2] , P. Kienle, W. Schott
Physik Department E12, Technische Universität München, D-85747 Garching, Germany

H. Geissel, G. Münzenberg[3]
Gesellschaft für Schwerionenforschung, D-64291 Darmstadt, Germany

Summary:

We propose to measure (d,^{3}He) spectra on light nuclei such as ^{7}Li and ^{12}C to search for η- and ω-nucleus bound states, and to deduce the meson mass shift in nuclei. The measurements are to be done using a deuteron beam from the GSI-SIS heavy-ion synchrotron at $T_d = 3.5$ GeV (η nucleus) and at $T_d = 3.8$ GeV (ω nucleus).

[1] Spokesperson
[2] co-spokesperson
[3] Local contact

1 INTRODUCTION

The purpose of the proposed experiment is to perform the recoilless production of η and ω mesons on nuclear targets using the (d,^{3}He) reaction, and to measure the meson-nucleus binding energies (and hence the meson mass shift in nuclei).

Recent theoretical developments on chiral symmetry breaking in QCD show that hadron properties in nuclei are closely related to the magnitude of the chiral quark condensate at finite nuclear density, and hence related to the non-trivial structure of the QCD vacuum[1].

In this context, there is currently a lot of interest in the investigation of how hadron properties may be modified in nuclear matter. At CERN, CERES[2] experiment, which measured e^+e^- invariant-mass spectra in heavy-ion collisions, have obtained tantalizing data which may be interpreted as ρ-meson mass being shifted (a few hundred MeV lighter) in hot dense nuclei. Similar results are reported by the HELIOS-3 experiment, which measured $\mu^+\mu^-$ invariant-mass spectra [3]. Experiments are also being planned at GSI (HADES)[4], and at RHIC (PHENIX)[5]. Even at normal nuclear density and in a small nuclear volume (such as ^{3}He), the ρ-meson mass reduction may be observed as suggested by a recent photoproduction experiment (TAGX)[6]. There is another on-going experiment at KEK which aims at measuring the ϕ meson mass shift in $p+A$ reactions[7]. Note that all these experiments measure l^+l^- ($l = e/\mu$) invariant mass spectra in order to address the question of meson mass shift, and that moving mesons probe the transient state of hot nuclei produced in violent nuclear collisions (except may be for the TAGX case).

We propose here an alternative and novel method of producing η and ω mesons near recoilless condition by using the (d,^{3}He) reaction. In this method, the target nucleus will remain near the ground state, and the produced meson will occupy some well-defined quantum levels (if the level widths are not too large as compared with the level spacing). As shown below, theoretical estimates show that both these mesons should exhibit negative mass shift in nuclear matter, and form meson-nucleus bound states. In the proposed experiment, the meson-nucleus binding energy can be determined unambiguously from the location of the bound-state peak in the (d,^{3}He) Q-value spectra, and the meson mass shifts can be inferred from the measured binding energies. The features of the proposed experiment are compared with those of heavy-ion experiments in Table 1.

Table 1: *The features of the proposed experiment are compared with those of heavy-ion experiments.*

	Proposed experiment	Heavy-ion experiments
Meson production	(d,^{3}He) *recoilless*	High-energy nuclear collisions
State of nuclear medium	Normal nuclear density (ground state)	Hot/dense, transient
State of the meson	$\sim$ bound	continuum
Mass measurement	Bound-state peak in Q-value spectra	l^+l^- invariant-mass spectra
Applicable to	π, η, ω, ...	vector mesons (ρ, ω, ϕ, ...)

Technically, the proposed experiment is identical to our recent GSI-SIS experiment, S160, in which we discovered deeply-bound pionic states in ^{208}Pb(d,^{3}He) reaction[8], and found that the pion mass becomes heavier by about 13% at the center of Pb nucleus[9, 10]. The same setup at the FRS can be used to perform the experiment, just by changing the incident deuteron energy and by tuning the FRS accordingly.

2 η/ω BINDING ENERGIES AND WIDTHS IN NUCLEI

Spontaneous chiral symmetry breaking in QCD provides non-trivial vacuum structure with non-zero chiral quark condensate $< \overline{q}q >$. The condensate depends on nuclear density ρ and temperature T, as shown in Fig. 1[14]. Hadron properties in nuclei are related to the partial restoration of this chiral symmetry at finite density.

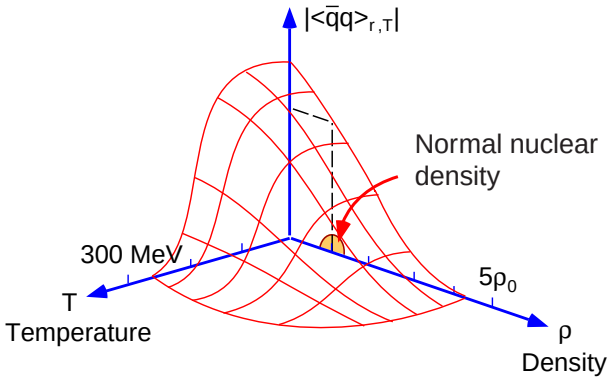

Figure 1: *Density and temperature dependence of quark condensate.*

The η meson is a member of the SU(3) octet of pseudoscalar mesons; this is at the same time believed to be one of the Nambu-Goldstone bosons of the spontaneous chiral symmetry breaking. The in-medium behaviors of π and K mesons, which are also Nambu-Goldstone bosons, have been reasonably well understood from scattering as well as mesonic-atom data. The behavior of η in nuclei is not well understood experimentally. In particular, the existence of η bound state in nuclei has been suggested and has been investigated for a decade[12], but not discovered up to now.

A recent lattice calculation[15] showed that η and η' meson masses become lighter at high temperature; for example, $m_{\eta'}(T = 0.75T_c)/m_{\eta'}(T = 0) = 0.86 \pm 0.02$ (η mass shift is smaller, but still appreciable). Although we cannot infer the density dependence of η mass from the results of lattice calculations, we expect that the shift is negative.

The problem of vector meson mass shift in nuclear matter is being actively studied by many authors. For example, in QCD sum rules, the vector meson mass shift is related to the ratio of quark condensate in nuclear matter $< \overline{q}q >_\rho$ and that in vacuum $< \overline{q}q >_0$, and is estimated to be[11]

$$\frac{m_{\rho/\omega}}{m_{\rho/\omega}(0)} = 1 - (0.16 \pm 0.06)\frac{\rho}{\rho_0}, \qquad \frac{m_\phi}{m_\phi(0)} = 1 - (0.15 \pm 0.05)y\frac{\rho}{\rho_0}, \tag{1}$$

where

$$y = \frac{2 < \overline{s}s >_N}{< \overline{u}u + \overline{d}d >_N} = 0.1 \sim 0.2. \tag{2}$$

The negative ω mass shift of $\sim 16\%$ at $\rho = \rho_0$ implies that the real part of the ω potential in normal nuclear matter is attractive and amounts to ~ -115 MeV (of course with a large uncertainty of ~ 30 %). Other authors[13, 18] also predict negative mass shift for ω.

2.1 η-nucleus: binding energies and widths

We now try to estimate the η-nucleus binding energies and widths. Recently, there exist three estimates on the ηN scattering length, two of which agree fairly well with each other:

$$\begin{aligned} a_{\eta N} &= (0.717 \pm 0.030) + i(0.263 \pm 0.025)\text{fm} \quad [16], & (3)\\ &= (0.751 \pm 0.043) + i(0.274 \pm 0.028)\text{fm} \quad [17], & (4)\\ &= 0.52 + i0.25\text{fm} \quad [12]. & (5) \end{aligned}$$

The lowest-order η-nucleus optical potential can be estimated as

$$V_\eta = -\frac{4\pi}{2\mu}\left(1 + \frac{m_\eta}{M_N}\right) a_{\eta N}\rho(\vec{r}), \tag{6}$$

where μ is the reduced mass of η and is $\sim m_\eta$ for heavy nuclei, M_N is the nucleon mass, and ρ is the nuclear density. For an illustrative purpose, let us take $\mu = m_\eta = 547$ MeV, $M_N = 939$MeV and $\rho_0 = 0.17\text{fm}^{-3}$ and $a_{\eta N} = 0.717 + 0.263i$fm. We then obtain

$$V(r) = -(86 + 32i)\rho(r)/\rho_0\text{MeV}, \tag{7}$$

which is strongly attractive. The imaginary part $W = -\Gamma/2$ is appreciable, but is small enough compared with the real part.

The η-nucleus binding energies and widths for various nuclei were calculated in a conventional way by solving the Klein-Gordon equation. A Woods-Saxon form of nuclear density profile was used, where nuclear radii and diffuseness were respectively taken to be $R = 1.18A^{1/3} - 0.48$ fm and $a = 0.5$ fm. The results are shown in Table 2. Note that

Table 2: *A-dependence of the η-nucleus binding energies and widths (for parameter choices, see text).*

A	1s		2p		3d	
	B.E.(MeV)	Γ (MeV)	B.E.(MeV)	Γ (MeV)	B.E.(MeV)	Γ (MeV)
5	-12.5	28.4				
6	-17.5	33.6				
10	-32.5	46.7				
12	-38.0	50.9	-2.50	28.6		
16	-46.4	57.0	-11.8	38.0		
20	-52.3	60.9	-19.6	44.5		
40	-66.7	68.2	-41.4	59.3	-15.9	48.6

$|\text{B.E.(1s)}| > \Gamma/2$ for all cases (except for $A = 5$), hence the bound-state peak should be clearly observable, well separated from the quasi-free continuum.

From the point of view of the bound-state peak search, light ($A < 12$) nuclei are favorable, since 1) the widths are small, so that the peak-to-background ratio is better, and 2) the peak structure is simple because there is only one bound state. Target choice will be discussed in detail in later sections.

2.2 ω-nucleus: binding energies and widths

The ω-nuclear binding energies and widths can be calculated in a similar way, once the potential is given. In the following estimate, the real part of the potential was set to be $-100\rho(r)/\rho_0$ MeV, based on Eq.1. The estimate of the imaginary part is difficult, since most of the authors who predict meson mass shift do not provide the width estimate. We chose imaginary part to be $W = -70\rho(r)/\rho_0$ MeV, based on a recent study by Klingl *et al.* [18] who showed ω lifetime τ_ω at $\rho = \rho_0$ to be $\sim$ 1.5 fm/c (which we interpreted as $W = -\Gamma/2 = -1/2\tau \sim -70$ MeV). The A-dependence of the binding energies and width are shown in Table 3. As shown, the widths (relative to the binding energies) are larger than the η case. Again, the results shown herein is subject to theoretical uncertainties, but we find that light nuclear targets are favorable in terms of the simplicity of the spectra and of S/N.

Table 3: *A-dependence of the ω-nucleus binding energies and widths.*

A	1s		2p	
	B.E.(MeV)	Γ (MeV)	B.E.(MeV)	Γ (MeV)
5	-24.1	85.7		
6	-30.7	96.0		
10	-48.8	119.8	-9.94	84.4
12	-55.0	127.2	-17.6	94.0
16	-64.1	138.0	-30.2	108.2

3 THE (d,^{3}He) REACTION: KINEMATICS AND CROSS SECTION

3.1 Recoil momentum vs deuteron kinetic energy

In Fig. 2, we plot the momentum transfer q vs incident deuteron kinetic energy T_d of the ^{7}Li(d,^{3}He)$^6_\eta$He (left panel) and ^{7}Li(d,^{3}He)$^6_\omega$He (right panel) reactions. The curves for other light nuclei would be similar to these. As shown, the recoil-free production of η is possible at GSI-SIS where the maximum deuteron kinetic energy T_d^{max} is 3.8 GeV. Although the production of ω at $q = 0$ is not possible at GSI-SIS, the recoil momentum q is about $\sim$ 250 MeV/c at $T_d = T_d^{max}$, not much larger than the nuclear Fermi momentum, so that there should be a finite probability of bound-state formation.

3.2 Cross section estimate - Green function approach

We estimate the reaction cross section on a nucleus target by using the response function:

$$\left(\frac{d^2\sigma}{d\Omega dE}\right)_{dA\to^3He(A-1)+\eta/\omega} = \left(\frac{d\sigma}{d\Omega}\right)^{lab}_{dp\to^3He+\eta/\omega} \times \sum_{l_{\eta/\omega},j_n,J} S(E) \qquad (8)$$

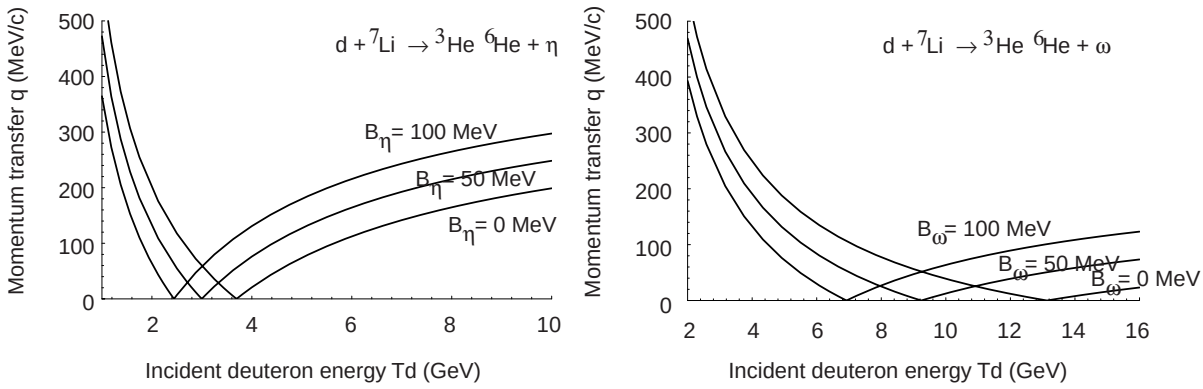

Figure 2: *The momentum transfer q vs incident deuteron kinetic energy T_d of the $^7Li(d,^3He)^6_\eta$He (left) and $^7Li(d,^3He)^6_\omega$He (right) reactions.*

Table 4: *Kinematical values for $^7Li(d,^3He)$ reaction at zero degree for the proposed η (left) and ω (right) production near the recoilless conditions.*

	η		ω	
Target nucleus	^{7}Li		^{7}Li	
Threshold T_d (GeV)	0.736		1.062	
Recoilless T_d in $d^7\text{Li} \rightarrow ^3$ HeX (GeV)	3.694		13.136	
Proposed T_d (GeV)	3.5		3.8	
p_d (GeV/c)	5.04		5.36	
$N_{eff}(s_{1/2})$	3.16×10^{-2}		6.80×10^{-3}	
$N_{eff}(p_{3/2})$	0.41×10^{-4}		0.98×10^{-3}	
$N_{eff}(total)$	3.16×10^{-2}		7.78×10^{-3}	
Meson Binding Energy (MeV)	0	15	0	30
Q value (GeV)	0.54745	0.53245	0.78194	0.75194
q (MeV/c)	14.6	2.5	265	229
$(p/z)_{^3\text{He}}$ (GeV/c)	2.512	2.520	2.546	2.564

where $\left(\frac{d\sigma}{d\Omega}\right)^{lab}_{dp\to{}^3\mathrm{He}+\eta/\omega}$ is the elementary cross section in the laboratory frame. A comprehensive and consistent approach to calculate the response function $S(E)$ for a system with a large imaginary potential was formulated by Morimatsu and Yazaki[23]. This method uses the Green function $G(E;r,r')$;

$$S(E) = -\frac{1}{2\pi} Im \sum_{M,m_s} \int d^3r d\sigma d^3r' d\sigma' f^{\dagger}(\vec{r},\sigma) G(E;r,r') f(\vec{r'},\sigma'). \tag{9}$$

We define $f(\vec{r},\sigma)$ as;

$$f(\vec{r},\sigma) = \chi^*_f(\vec{r}) \xi^*_{\frac{1}{2},m_s}(\sigma) [Y^*_{l_{\eta/\omega}}(\hat{r}) \otimes \psi_{j_p}(\vec{r},\sigma)]_{JM} \chi_i(\vec{r}) \tag{10}$$

where χ_i and χ_f respectively denote the projectile and the ejectile distorted waves, $\phi_{\eta/\omega}$ is the meson bound state wavefunction, ψ is the proton hole wavefunction and ξ is the spin wavefunction of the proton in the target nucleus; the numerical values of $S(E)$ were evaluated by using the eikonal approximation as in the case of deeply-bound pionic atom[19] (see Fig.3). In this formulation, we can obtain the effective numbers, which have been used to calculate the pionic atom formation cross sections, approximately as;

$$N_{eff} \sim \int S(E) dE \tag{11}$$

The effective proton numbers for η and ω production on ^{7}Li at the proposed incident energy are shown in Table 4, where $N_{eff}(s_{1/2})$, $N_{eff}(p_{3/2})$ and $N_{eff}(total)$ respectively denote the contribution of the $s_{1/2}$ protons in ^{7}Li, $p_{3/2}$ proton contribution, and total.

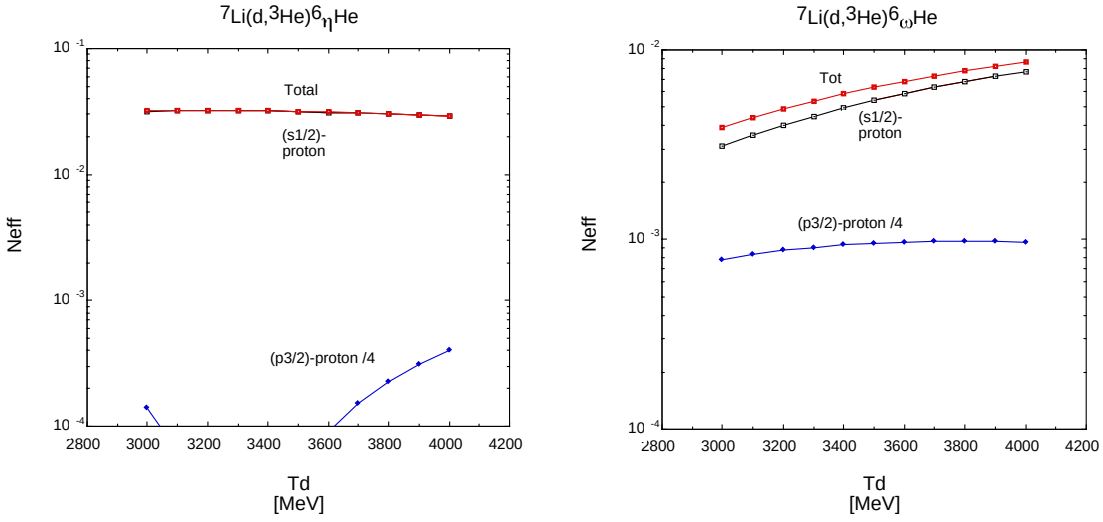

Figure 3: *Effective proton number N_{eff} for ^{7}Li target as a function of incident deuteron kinetic energy: η production (left) and ω production (right).*

3.2.1 η production cross section at $T_d \sim 3.5$ GeV

The elementary cross section for η production can be inferred from the energy dependence of the $pd \rightarrow {}^3\mathrm{He}\eta$ cross section measured at SATURNE (Fig. 4 [20]). At $T_p = 1.75$ GeV, the energy corresponding to the c.m. energy of the recoilless η production in the $dp \rightarrow {}^3\mathrm{He}\eta$ reaction, the c.m. cross section $(d\sigma/d\Omega)_{cm}$ is 3 nb/sr. This can be translated to the dp laboratory-frame cross section via

$$\frac{d\sigma}{d\Omega}_{lab} = \left(\frac{p_{lab}(^3\mathrm{He})}{p_{cm}(^3\mathrm{He})}\right)^2 \frac{d\sigma}{d\Omega}_{cm}, \tag{12}$$

and we estimated the elementary cross section to be ~ 150 nb/sr. By using the N_{eff} tabulated in Table 4, the $^7\mathrm{Li(d,}^3\mathrm{He)}^6_\eta\mathrm{He}$ cross section is estimated to be ~ 4.7 nb/sr.

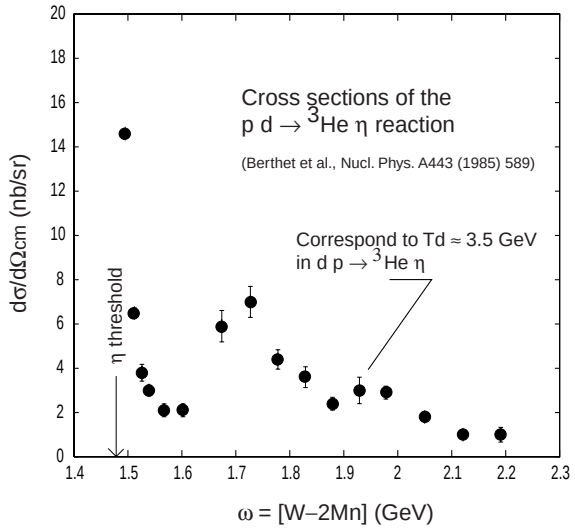

Figure 4: *The $\theta_\eta = 180°$ excitation function of the $pd \rightarrow {}^3\mathrm{He}\eta$ reaction as a function of the total c.m. energy minus two nucleon masses, taken from Ref.[20].*

3.2.2 ω production cross section at $T_d \sim 3.8$ GeV

The near-threshold $pd \rightarrow {}^3\mathrm{He}\omega$ data at SATURNE (Fig. 5 [21]) were used to estimate the elementary cross section of ω production. The dp reaction at $T_d \sim 3.8$ GeV correspond to $T_p \sim 1.9$ GeV ($p_\omega^{cm} = 625$ MeV/c) in Ref.[21], where the c.m. cross section is given to be ~ 7 nb/sr. By using Eq.12, we can estimate the elementary cross section to be ~ 450 nb/sr. Multiplied by N_{eff} (Table 4), we obtain an estimate for the $^7\mathrm{Li(d,}^3\mathrm{He)}^6_\omega\mathrm{He}$ cross section at $T_d \sim 3.8$ GeV to be about ~ 3.5 nb/sr.

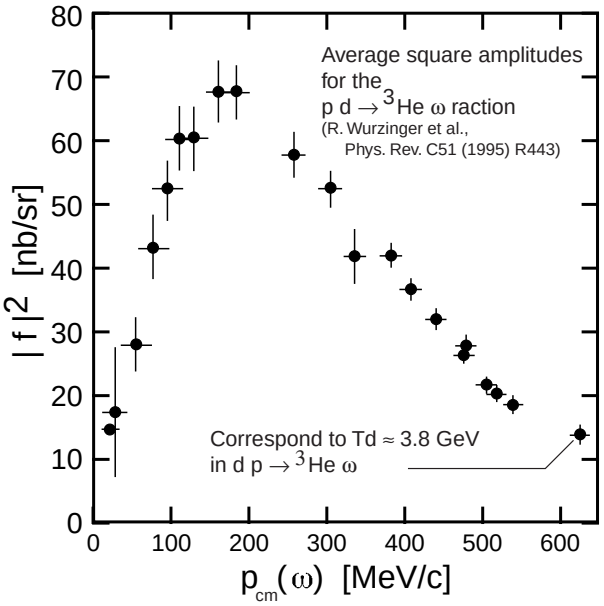

Figure 5: *Average squared amplitudes* $|f_\omega|^2 = \frac{p_p^{cm}}{p_\omega^{cm}} \left(\frac{d\sigma}{d\Omega^{cm}}\right)$ *for the* $pd \rightarrow^3$ Heω *reaction as a function of* p_ω^{cm} *for* $\theta_\omega^{cm} = 180°$, *taken from Ref.[21].*

3.3 Expected spectra

3.3.1 Spectra calculated using Green function method

In Figs. 6-7, we show the calculated spectra using Green function method described above. Since the experimental resolution is much better than the natural widths of these states, it was not folded in.

Because of small momentum transfer in the case of η production, the $(s_{1/2})_p^{-1}(1s)_\eta$ component contributes dominantly to the Q-value spectrum, and a clear peak appears corresponding to the $1s$ bound state of η. The next dominant contribution is the $(p_{3/2})_p^{-1}(p)_\eta$ component, which makes a small bump in the unbound region. Contributions of other components such as $(s_{1/2})_p^{-1}(p)_\eta$ or $(p_{3/2})_p^{-1}(1s)_\eta$ can be safely ignored.

The situation is different in the case of ω production, for which the momentum transfer is appreciable at the GSI-SIS energy region. Although the $(s_{1/2})_p^{-1}(1s)_\omega$ component has a peak at the expected position of $1s$ bound state as shown in Fig. 7, the quasi-free ω production contributions ($(s_{1/2})_p^{-1}(p)_\omega$, $(s_{1/2})_p^{-1}(d)_\omega$, etc.) is larger. When all components are added, the $1s$ bound-state peak is no longer clearly visible.

3.3.2 Background considerations

In order to generate realistic Q-value spectra including background, we considered the following:

1. The continuum background level was estimated by using the published spectra of η/ω production.

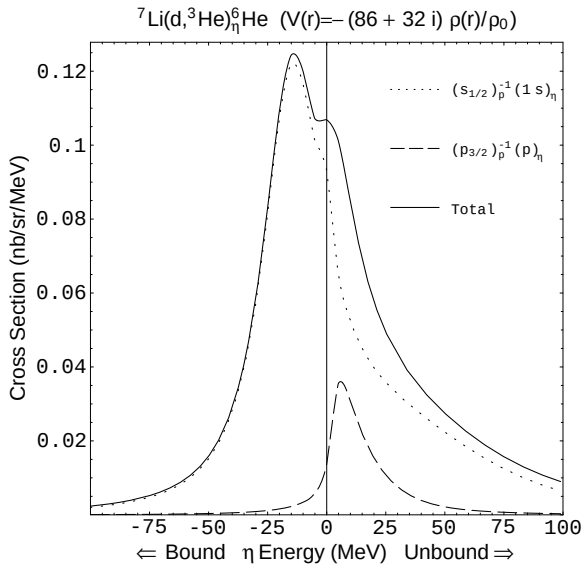

Figure 6: *The expected spectra of the* $^7Li(d,^3He)$ *reaction (*η *region, without adding background), for* $V(r) = -(86 + 32i)\rho(r)/\rho_0$MeV.

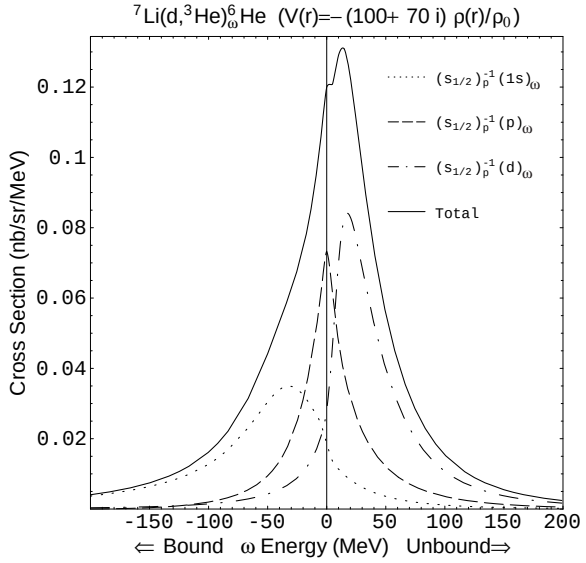

Figure 7: *The expected spectra of the* $^7Li(d,^3He)$ *reaction (*ω *region, without adding background), for* $V(r) = -(100 + 70i)\rho(r)/\rho_0$MeV.

- The background for η production was estimated by using the data of Berthet *et al.* (figure (1)b of Ref. [20]). By counting the number of events shown, and by relating the counts to the tabulated c.m. cross section, we estimated the c.m. continuum background level to be $\sim$ 0.09nb/sr/MeV at $T_p = 2$ GeV ($T_d = 4$ GeV). In the (d,^{3}He) laboratory frame, this would correspond to $d^2\sigma/dEd\Omega_{lab} \sim 4.5$ nb/sr/MeV.
- The $pd \rightarrow ^3$ He$\pi^+\pi^-$ data near the η threshold by Mayer *et al.*[22] show that the continuum background due to $\pi^+\pi^-$ production is flat across the η production threshold. We therefore ignored the possible Q-value dependence of the continuum background.
- The background for ω production was estimated by using the data of Wurzinger *et al.* (figure 1 of Ref. [21]), which indicate a c.m. continuum background level of $\sim$ 0.5 nb/sr/MeV at $T_p = 1.9$ GeV ($T_d = 3.8$ GeV). In the (d,^{3}He) laboratory frame, this would correspond to $d^2\sigma/dEd\Omega_{lab} \sim 33$ nb/sr/MeV.

2. In order to evaluate the continuum background in nuclear target cases, we need to calculate the distortion effects of deuteron and ^{3}He in target nucleus. For this purpose, we summed up the effective numbers for all final state configurations of proton-hole and mesonic states, and multiplied it to the continuum background in elementary process. This total effective number is expected to be good estimation of distortion effects to projectile and ejectile. And this is also expected to be consistent with the estimation of signal cross sections.

3. In the present reaction, we may have additional background due to ^{3}He formation without meson production (such as due to coalescence). Composit particle production with a few GeV protons incident on nuclear targets was studied by Tokushuku *et al.* [24] at KEK; in Fig. 1 (a) of ref. [24], we find the deuteron spectra of $Al(p,d)$ reaction at $T_p = 3GeV$. We estimated the order of magnitude of background using this data. By extrapolating the data to $p_d \sim 4GeV/c$, corresponding to our region of interest, we found that the cross section is around $10^{-9}[nb/(MeV/c)sr]$. This is extremely tiny compared to the expected signal and is totally negligible.

4 EXPERIMENTAL SETUP

We propose to use the same FRS setup (Fig.8) as used in our recent S-160 experiment (deeply-bound pionic atom). The target materials are ^{7}Li (^{nat}Li) and ^{12}C. Since the signal peak widths are expected to be large, we need not optimize the experiment for achieving high resolution. We can thus use thick ($\sim$ 1g/cm^2) targets. For calibration, we use a $\sim$ 1g/cm^2 $(CH)_n$ target; a discrete peak of $dp \rightarrow ^3$ He $+ \eta/\omega$ can be used to calibrate the energy scale and also to check the cross section.

The use of (d,^{3}He) reaction is essential to study recoilless meson production, since the magnetic rigidities of the incident deuteron and ejected ^{3}He are different, even when $q = 0$ (i.e., $p_d = p_{^3\mathrm{He}}$). Thus, the beam deuterons are dumped in the first bending magnet of FRS, and we can measure clean ^{3}He Q-value spectra[4] . The background protons due to deuteron

[4] The recoilless meson production is also possible by using the (p,d) reaction, but in this case, the magnetic

breakup can be eliminated as in the case of S-160, by setting high discriminator thresholds in trigger counters, and also by lowering the chamber high voltages, so that the chambers are sensitive to ^{3}He but not sensitive to protons. If the background proton rate is higher than expected at S2, we can move the drift chambers to S4 and analyze momenta between S2 and S4.

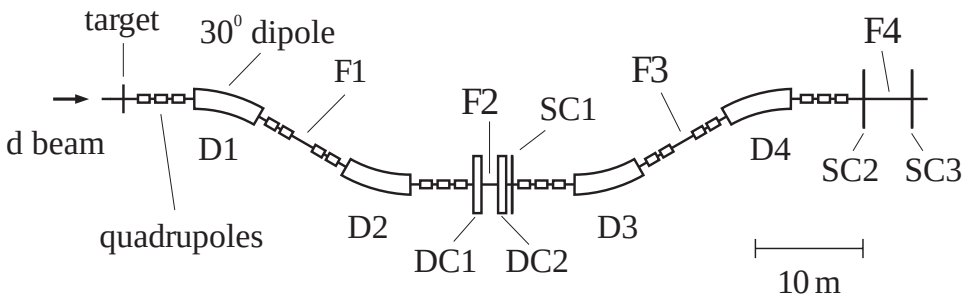

Figure 8: *Layout of the proposed experiment at FRS is the same as in S-160 (deeply-bound pionic atom experiment). At the mid-focal plane (F2) two sets of drift chambers (DC1 and DC2) and a segmented scintillation counter (SC1) are installed. At the final focal plane (F4) other scintillation counters (SC2 and SC3) are placed. The 1st and 2nd bending sections (D1 and D2) provide a dispersive focal plane for momentum analysis and the 3rd and 4th sections (D3 and D4) transport the ^{3}He ions to F4.*

The yield estimate assumes

$$\begin{aligned} I_d &= 3 \times 10^{10}/\mathrm{sec}, \\ N_{target} &= 9 \times 10^{22}\mathrm{atoms/cm}^2 \quad (1\mathrm{g/cm}^2 \ {}^7\mathrm{Li}), \\ \Omega &= 2.5 \times 10^{-3}\mathrm{sr} \quad (\Delta\theta_\mathrm{x} \sim \pm 40\mathrm{mr},\ \Delta\theta_\mathrm{y} \sim \pm 20\mathrm{mr}). \end{aligned}$$

The solid angle is larger than in the case of S160 since we would use target station 2 which is at 1.1m distance from the first quadrupole instead of 2m as in S160. For this target position we have an ion-optical setting (developed by Arnold Schroeter as backup version for our pbar/K- production experiments) with 4.2cm/% dispersion i.e. $\sim 60\%$ dispersion of the S160 value. Fig.9 shows the relationship beteen the η/ω energy and the ^{3}He position on the focal plane, with the dispersion of 4.2 cm/%. Since our chambers have active region of ± 10 cm and the acceptance is known to be flat within $\sim \pm 5$ cm, we can cover the η region of interest ($\pm$100MeV) in two FRS settings, and the ω region of interest ($\pm$200MeV) in two or three FRS settings.

The expected spectra for 100 hours of running (if two or three different FRS settings are needed as discussed above, the actual running times are correspondingly longer) are shown in Fig. 10. In both cases, the η/ω production peaks can be identified with sufficient statistical significance. For the particular choice of potential parameters we used to generate these spectra, the η bound state can be clearly identified. However, the ω bound state peak is

rigidities of the projectile and ejectile are the same at $q = 0$. The beam protons will be focussed on the FRS focal plane, making the measurement impossible.

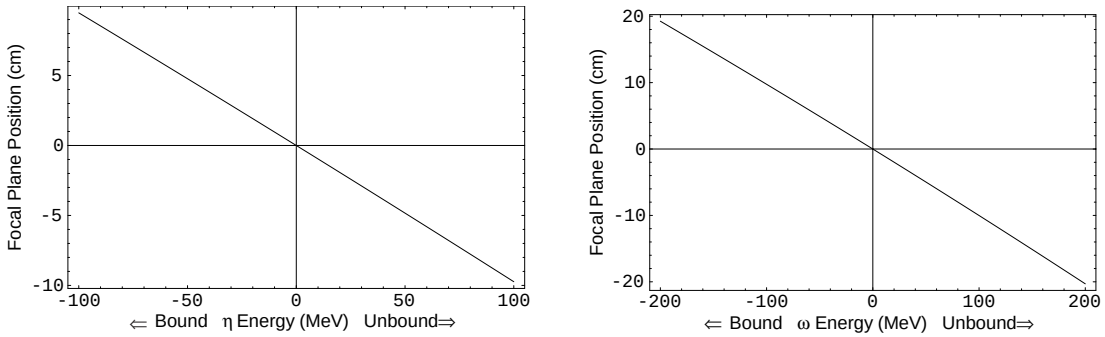

Figure 9: *Left: η energy (MeV) vs ^{3}He position on the focal plane (cm). Right: ω energy (MeV) vs ^{3}He position on the focal plane (cm).*

buried in the tail of quasi-free continuum. If the imaginary part of the $\omega - N$ potential is in fact smaller, we should be able to identify the bound-state peak.

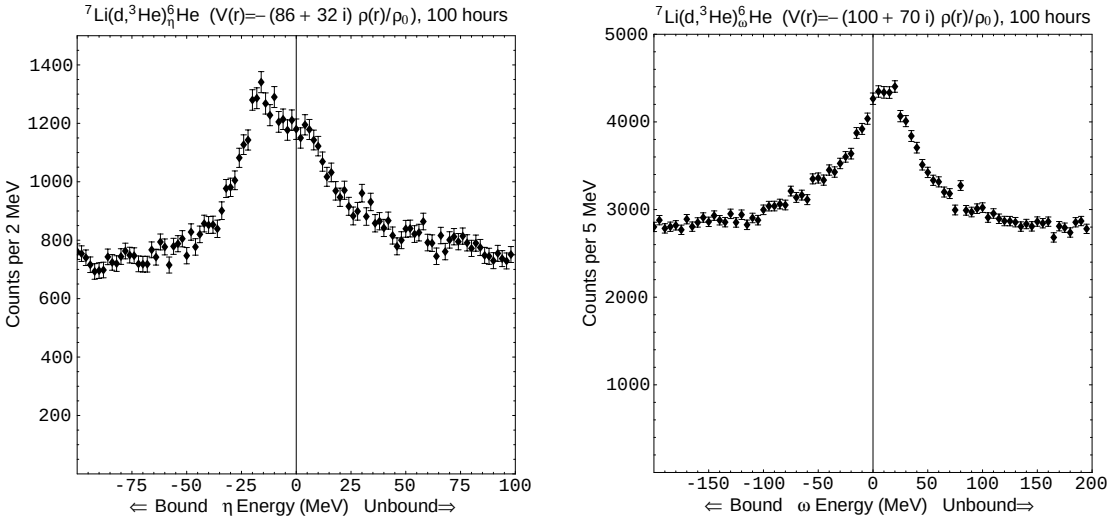

Figure 10: *Left: Expected spectrum of $^7(d,^3He)^6_\eta He$ for 100 hours of running at FRS. Right: Expected spectrum of $^7(d,^3He)^6_\omega He$ for 100 hours of running at FRS.*

5 BEAM TIME REQUEST

Based on the above estimates, we request the beam time as follows:

	η	ω
T_d (GeV)	3.5	3.8
Shake down (hours)	50	
Calibration run (with $(CH)_n$) (hours)	25	25
Physics run (with carbon and Li, 2-3 FRS settings) (hours)	$100 \times 2 \times 2 = 400$	$100 \times 2 \times 3 = 600$
Total (hours)	1100	

References

[1] See, for instance, T. Hatsuda and T. Kunihiro, Phys. Rep. 247 (1994) 241; G. E. Brown and M. Rho, Phys. Rep. 269 (1996) 333.

[2] G. Agakichev et al., Phys. Rev. Lett. 75 (1995) 1272; Th. Ullrich, Nucl. Phys. A610 (1996) 317c.

[3] M. Masera, Nucl.Phys. A590 (1995) 93c.

[4] HADES home page:
`http://piggy.physik.uni-giessen.de/hades/`.

[5] PHENIX home page:
`http://www.rhic.bnl.gov/export1/phenix/WWW/phenix_home.html`.

[6] K. Maruyama, in Proc. Int. Conf. on Quark Lepton Physics (Osaka), to appear in Nucl. Phys. A (1997).

[7] KEK E325 home page:
`http://kupns1.scphys.kyoto-u.ac.jp/~yokkaich/phi/pub/E325_project.html`.

[8] T. Yamazaki *et al.*, Z. Phys. A355 (1996) 219.

[9] T. Yamazaki *et al.*, submitted to Phys. Lett. B.

[10] T. Waas, R. Brockmann, W. Weise, hep-ph/9704397.

[11] T. Hatsuda and S.H. Lee, Phys. Rev. C 46 (1992) R34; Invited talk at the 25th INS International Symposium on Nuclear and Particle Physics with High-Intensity Proton Accelerators, (Dec. 3-6, 1996, Tokyo, Japan.)

[12] N. Willis et al., Phys.Lett.B406(1997)14

[13] X.Jin, D.B.Leinweber, Phys. Rev. C52 (1995) 3344

[14] T. Hatsuda and T. Kunihiro, Phys. Rev. Lett. 55 (1985) 158; W. Weise, Nucl. Phys. A553 (1993) 59c.

[15] S. Hioki, hep-lat/9702007.

[16] M. Batinić *et al.* nucl-th/9703023.

[17] A.M. Green, S. Wycech, Phys. Rev. C55 (1997) R2167.

[18] Kringl, Kaiser, Weise, hep-ph/9702240, hep-ph/9704398.

[19] H. Toki, S. Hirenzaki and T. Yamazaki, Nucl. Phys. A530 (1991) 679.

[20] P. Berthet *et al.*, Nucl. Phys. A443 (1985) 589.

[21] R. Wurzinger *et al.*, Phys. Rev. C51 (1995) R443.

[22] B. Mayer *et al.*, Phys. Rev. C53 (1996) 2068.

[23] O. Morimatsu and K. Yazaki, Nucl. Phys. A435 (1985) 727; Nucl. Phys. A483 (1988) 493.

[24] K. Tokushuku, *et al.*, Phys. Lett. 235B (1990) 245.